IEEE Access
Multidisciplinary | Rapid Review | Open Access Journal

Received January 30, 2020, accepted March 1, 2020, date of publication March 10, 2020, date of current version March 20, 2020.

Digital Object Identifier 10.1109/ACCESS.2020.2979866

Approximation of the Nonlinear B-H Curve by Complex Exponential Series

MARTIN DADIĆ, MARKO JURČEVIĆ, (Member, IEEE), AND ROMAN MALARIĆ
Faculty of Electrical Engineering and Computing, University of Zagreb, 10 000 Zagreb, Croatia

Corresponding author: Marko Jurčević (marko.jurcevic@fer.hr)

This work was supported by the Croatian Science Foundation under the project Metrology infrastructure for support of the intelligent power grid under Grant IP-2019-04-7354.

ABSTRACT The paper presents an accurate and simple method for the approximation of the nonlinear B-H curves using expansion into complex exponential series. The least-squares fit of the model is obtained by the application of the Moore-Penrose pseudoinverse. Due to the completeness of the orthogonal basis of the approximation, any desired accuracy can be achieved with increasing the number of terms. Using the measurements acquired by an automated system based on the PXI digitizer boards, the feasibility of the method is proved.

INDEX TERMS B-H curve, non-linear magnetics, complex exponential series, digitizers.

I. INTRODUCTION

The numerical methods like finite element method (FEM) need accurate expressions representing the *B-H* curve. Although it is possible to introduce hysteresis models like Jiles-Atherton [1] or Preisach model of ferromagnetic materials into the FEM analysis [1]–[14], it is still relevant to use the single-valued *B-H* curve in such an analysis. For the magnetically soft materials, the hysteresis loops are relatively narrow. Therefore, the single-valued *B-H* curve represented by the initial magnetization curve adequately characterizes such materials in many applications like the calculation of the magnetic field in motors and generators [4]. Consequently, the computational effort is reduced, and the speed of the calculations is increased. In such a case, the losses are usually estimated using analytical formulae, while the nonlinear problem is solved using the Newton-Raphson or successive substitution method [15]–[17]. The accurate modeling of single-valued *B-H* curve is also important in equivalent magnetic circuit modeling [18]. Moreover, the anhysteretic, single-valued *B-H* models [19], [20] are important in the analysis of magnetic recording systems [21], while the anhysteretic *B-H* curve is the basis of the Jiles-Atherton model of the magnetic hysteresis [22].

The analytical expressions used for the single-valued representation of a *B-H* curve are traditionally based on empirical formulas [23]–[25] or power series representation [26], [27]. The other approaches include representation by hyperbolas [26], transcendental functions [26], exponential series or sums of exponentials [28], [29], and rational functions [30]–[32]. The possibility of very accurate modeling of the whole *B-H* curve (including Rayeigh region and saturation knee) launched the approximation using Fourier series [26], [33]. The Fourier series approximation converges well, and any desired accuracy can be achieved [26]. However, the calculation of Fourier coefficients [34] needs the integration of the *B-H* curve, which is available only at discrete (measured) points. Thus, the numerical integration and the interpolation of the curve between the points must be applied [33]. The Fourier analysis is widely applied in the time to frequency transformations and representation of signals and functions [35]. In the wider context, the representation of the discrete-time systems and signals using the z-transformation and finite impulse response (FIR) models is a well-established discipline [35], [36]. Applying the Fourier transformation to the Lth-order FIR system approximation

$$A(z) = \sum_{k=0}^{L} a_k z^{-k} \tag{1}$$

yields

$$z = e^{\frac{j2\pi f}{\chi}} \tag{2}$$

$$A(f) = \sum_{k=0}^{L} a_k e^{-\frac{j2\pi fk}{\chi}} \tag{3}$$

The associate editor coordinating the review of this manuscript and approving it for publication was Wuliang Yin.

which is a sum of complex exponentials. Here, f denotes frequency, z is complex variable in z-transformation, a_r is set of coefficients χ is sampling frequency, and A is the approximation of the system function. The Fourier transform of the FIR model is a periodic function of frequency with period χ [35]. In the sequel (section 3) it will be demonstrated that the proposed complex exponential series form the complete orthogonal system. The methods for the determination of the coefficients a_r are well established [37], [38] and thus can be applied in the proposed modeling of *B-H* curve. While the system modeling usually imposes additional requirements on the causality [39] or the real character of the coefficients a_r, these requirements are weakened in the *B-H* curve modeling, which allows direct application of the unconstrained least-squares methods in the evaluation of the coefficients.

The main purpose of this paper is to present a method for the approximation of the nonlinear *B-H* curves using expansion into complex exponential series, where the least-squares fit to the data is obtained by the application of the Moore-Penrose pseudoinverse. The proposed approximation easily allows use of the non-uniformly sampled points in the measured *B-H* curve. Moreover, it is analytically derivable, which can be applied in the calculation of the magnetic permeability and the energy stored in the magnetic material [27], [28].

The paper is organized as follows: in Section II the measurement system based on NI 4461 DAQ cards is described. Section III presents the proposed method for the *B-H* curve approximation. Section IV gives the results. Finally, Section V are conclusions.

II. MEASUREMENT SYSTEM

The measurement system is based on commercial *National Instruments* PXI modular measurement system equipped with digitizer board, *Toellner* TOE 7621 four-quadrant power supply working in voltage-controlled mode, R-C integrator, precise shunt and a ferromagnetic coil test sample.

The NI-PXI4461 (named hereafter as NI4461) module is used as a digitizer unit placed in PXI chasis. It is a dynamic signal acquisition device equipped with two simultaneously sampled input and output channels, integrating sigma-delta A/D and D/A converters, both with 24-bit resolution and sampling rates up to 204.8 kS/s. The PXI system generates the excitation signal, which is fed to the input of the TOE 7621 power supply. The amplitude of the excitation current is measured as voltage drop present on the shunt R_s. The resistance of the shunt is considered constant, independent of the ambient temperature and applied voltage.

The control of measurement process and measured data processing is performed in LabVIEW environment. Aim was to use fully automated measurement of the first magnetization curve to prepare measured data for export in a format ready for the import to a computer program for the B-H curve approximation.

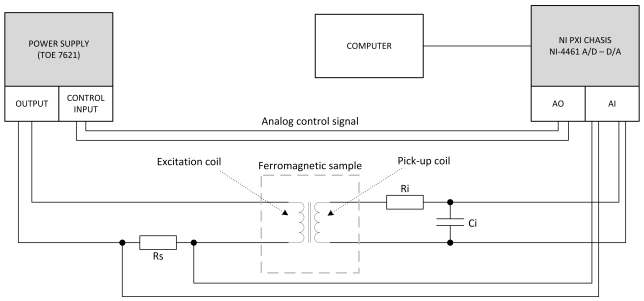

FIGURE 1. Block diagram of the measurement system.

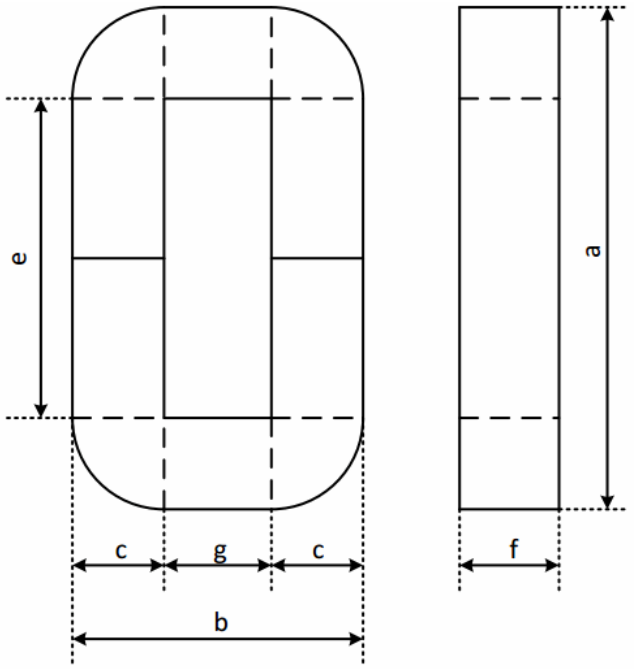

FIGURE 2. C-core specimen.

Fig. 1 presents the block diagram of the measurement system.

The measurement set-up is based on the IEEE standard procedures for magnetic cores, where the RC integrator is connected on the search (pick-up) coil. The single-valued initial *B-H* curve is measured using the locus points of the symmetric hysteresis cycles [40], [41]. Instead of using a ring core specimen, measurements were performed using a SU30 ferromagnetic C-core (*Iskra*). C-cores also have reasonably uniform flux density and therefore are useful for the *B-H* curve measurement [42]. Fig. 2 and Table 1 give the dimension of the core.

The number of turns was $N = 169$ in both coils, while the wire diameter was 0.3 mm. Using the Ampère's law, the magnetic field in the core is

$$H(t) = \frac{Nu_S(t)}{l_m R_S} \tag{4}$$

where l_m is the average length of the flux lines, and $u_S(t)$ is the voltage drop across the shunt resistor R_s.

TABLE 1. Dimensions of the core.

Dimension	Standard values [mm]
b	30
c	9.9
f	10.1
a	52.7
g	10
e	32.5

The magnetic flux density is

$$B(t) = \frac{R_i C_i}{NS} u_C(t). \tag{5}$$

Here, S denotes the cross-section of the coil, R_i is the resistor value of the RC integrator, C_i is the capacitance of the capacitor in the RC integrator, and $u_C(t)$ is the voltage across the capacitor C. Using the data from the Table 1, the cross-section and the average length of the flux lines is

$$S = c \cdot f = 9.388 \cdot 10^{-5}\ \mathrm{m}^2$$
$$l_m = 2(e+g) + c\pi = 0.116\ \mathrm{m}$$

In characterizing an analog-to-digital converter (ADC), one of the important parameters is the integral nonlinearity (INL). As this experiment was done at frequency of 20 Hz, work provided in [43] declares INL that is below 1 μV/V.

For simultaneous sampling of 1 V signal amplitude, input range $\pm$1V and sampling frequency of 51.2 kS/s, the NI4461 metrological characteristics are provided [44]:

- temperature coefficient of the magnitude is 7.4 μV/V$\cdot$K,
- temperature coefficient of the phase is 0.000008°/K,
- standard deviation of the magnitude of the voltage ratio is 2.3 μV/V,
- deviation of the magnitude of the voltage ratio from the nominal value is within $\pm$3 μV/V,
- phase deviation is under 16 μ°.

Following components:

- current shunt,
- integrator resistor,
- integrator capacitor

were measured in slow mode using the LCR Bridge Rohde & Schwarz (*Hameg*) HM8118, applying the average and 4-wire connection and the open-short calibration.

The resistance of the integrator resistor is
$R_\mathrm{i} = (382.93 \pm 0, 27)\ \mathrm{k}\Omega$.
The capacitance of the integrator capacitor is
$C_\mathrm{i} = (2.9752 \pm 0, 0176)\ \mu\mathrm{F}$.
The resistance of the current shunt is
$R_\mathrm{s} = (1.0084 \pm 0, 0041)\ \Omega$.

III. COMPLEX FIT

Let have the set of M measured pairs $(H_\mathrm{k}, B_\mathrm{k})$, $k = 0, \ldots M-1$, which satisfy

$$H_k \in [0, H_\mathrm{max}] \tag{6}$$
$$B_k \in [0, B_\mathrm{max}] \tag{7}$$

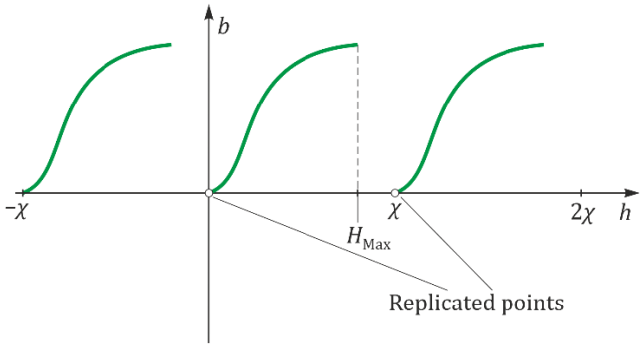

FIGURE 3. Non-overlapping replicas of the model.

Using the model representation given by the equation (3), we seek the representation of the sampled nonlinear curve using the approximation

$$b(h) = \sum_{k=0}^{L} \underline{a}_k e^{-\frac{j2kh\pi}{\chi}} \tag{8}$$

where b denotes the modeled magnetic flux density and h is the magnetic field strength. Moreover, $\{\underline{a}_k\}$ is a set of complex-valued coefficients, L is the order of the approximation, and χ is a parameter that defines the periodicity of the model in terms of the variable h.

The set of orthogonal functions

$$e^{-\frac{j2kh\pi}{\chi}} \tag{9}$$

form the complete orthogonal system. It can be seen using the substitution

$$z = e^{-\frac{j2h\pi}{\chi}} \tag{10}$$

where the expansion (8) yields the form of Laurent series. In this way the completeness of the proposed approximation follows from the completeness of Laurent series and Fourier series [35, §14.1 and §9.4].

The model (8) is periodic in h with the period χ, which is easily obtained using the substitution

$$h' = \chi + h \tag{11}$$

which yields

$$e^{-\frac{j2kh'\pi}{\chi}} = e^{-\frac{j2k\pi}{\chi}(\chi+h)} = e^{-\frac{j2kh\pi}{\chi}} \tag{12}$$

The impact of the periodicity of the model on the upper bound of the parameter χ can be illustrated with Figs. 3 and 4. In Fig. 3, H_max is lower than χ, and consecutive replicas of the model does not overlap. In Fig. 4, H_max exceeds χ and the consecutive replicas of the model overlap in the intervals H_ϑ. Thus, accurate modeling of the B-H curve cannot be achieved in the pink regions, since the model function cannot be uniquely defined for these regions. To ensure that the model does not overlap in h the parameter χ has to satisfy the condition:

$$\chi > H_\mathrm{max} \tag{13}$$

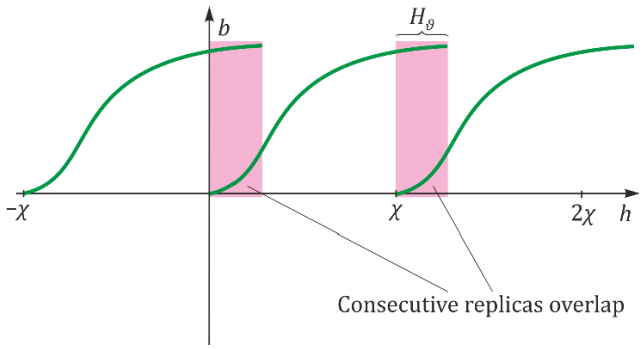

FIGURE 4. Overlapping replicas of the model.

Nevertheless, the experiments with the varying the parameter χ from $1.1H_{\max}$ to $2H_{\max}$ has shown that the quality of the approximation gradually degrades for χ lower than $1.5H_{\max}$. Therefore, in all further presented modeling the parameter χ was chosen to be

$$\chi = 2H_{\max} \tag{14}$$

It should be noted that the interval

$$\langle H_{\max}, \chi \rangle \tag{15}$$

forms the "don't care" interval, for which the approximated function b is not defined.

If we define column vectors

$$\mathbf{A} = \begin{bmatrix} \underline{a}_0 & \underline{a}_1 & \underline{a}_2 & \ldots\ldots & \underline{a}_{L-1} \end{bmatrix}^T \tag{16}$$

$$\mathbf{C}(h) = \begin{bmatrix} 1 & e^{-j2\pi h/\chi} & e^{-j\cdot 2\cdot 2\pi h/\chi} & \ldots\ldots & e^{-jL2\pi h/\chi} \end{bmatrix}^T \tag{17}$$

we can express the error function as [45], [46]

$$e(h) = b(h) - \mathbf{C}^T(h)\mathbf{A} \tag{18}$$

Here, T denotes vector transpose. Equation (13) can be expressed for M (B_k, H_k) pairs as

$$\mathbf{E} = \mathbf{D} - \mathbf{F}\mathbf{A} \tag{19}$$

where

$$\mathbf{E} = \begin{bmatrix} e(H_0) & e(H_1) & e(H_2) & \ldots\ldots & e(H_{M-1}) \end{bmatrix}^T \tag{20}$$

$$\mathbf{D} = \begin{bmatrix} B_0 & B_1 & B_2 & \ldots\ldots & B_{M-1} \end{bmatrix}^T \tag{21}$$

$$\mathbf{F} = \begin{bmatrix} \mathbf{C}(H_0) & \mathbf{C}(H_1) & \mathbf{C}(H_2) & \ldots\ldots & \mathbf{C}(H_{M-1}) \end{bmatrix}^T \tag{22}$$

The design problem is to minimize the sum of error squares:

$$e_W = \sum_{m=0}^{M-1} \|e(h_m)\|^2 \tag{23}$$

which can be expressed in matrix notation as:

$$\mathbf{F}\mathbf{A} \cong \mathbf{D} \tag{24}$$

In the sequel we use the mathematical equivalence of the least-squares problem (18) and the system of normal equations [47]

$$(\mathbf{F}^H\mathbf{F})\mathbf{A} = (\mathbf{F}^H\mathbf{D}) \tag{25}$$

Here, H denotes the Hermitian conjugate transpose operator.

Although it is tempting to solve (14) directly as

$$\mathbf{A} = \left(\mathbf{F}^H\mathbf{F}\right)^{-1}\mathbf{F}^H\mathbf{D} \tag{26}$$

it is impossible for $L \ll M$, since in this case $\mathbf{F}$ becomes ill-conditioned [37], and a direct solution will probably have large errors. Therefore we propose to solve the system using the matrix pseudoinverse.

For a $m \times n$ matrix $\mathbf{F}$, its pseudoinverse $\mathbf{F}^+$ gives the minimum-norm [48] solution to the least-squares problem

$$\mathbf{F}\mathbf{A} \cong \mathbf{D} \tag{27}$$

as

$$\mathbf{A} = \mathbf{F}^+\mathbf{D} \tag{28}$$

The explicit list of the properties of the Moore-Penrose (MP) pseudoinverse can be found in [47]. The calculation of the MP pseudoinverse is generally based on the singular value decomposition, which is efficiently implemented in LAPACK and also in LAPACK based MATLAB routine *pinv* (15).

Using the proposed approximation, the derivative of the b with respect to h is

$$\frac{\partial b}{\partial h}(h) = -j\frac{2\pi}{\chi}\sum_{k=1}^{L} k\underline{a}_k e^{-\frac{j2kh\pi}{\chi}} \tag{29}$$

from which the permeability can be expressed as

$$\mu = \frac{\partial b}{\partial h} \tag{30}$$

Remark: If the set of coefficients $\{\underline{a}_k\}$ would be restricted to real numbers, the magnitude of the model function would be even function of parameter h [26]. In line with the Whittaker-Shannon theorem this would impose a stronger condition on the parameter χ [49]–[51]:

$$\chi > 2H_{max} \tag{31}$$

IV. RESULTS

Using the proposed method, the approximation of a measured B-H curve was calculated. The measurements were performed using the setup from Section 2. In the origin of the b-h plane, the point (0,0) was added to measured pairs. The overall number of data point was $M = 1274$, while the order of the approximation was $L = 100$. Since the method allows application of the non-equidistant sampling of the data points (in h- or b-axis), the measurements were done with denser sampling for lower values of the magnetic flux densities. The algorithm for the approximation was programmed in MATLAB, and the pseudoinverse was calculated using the

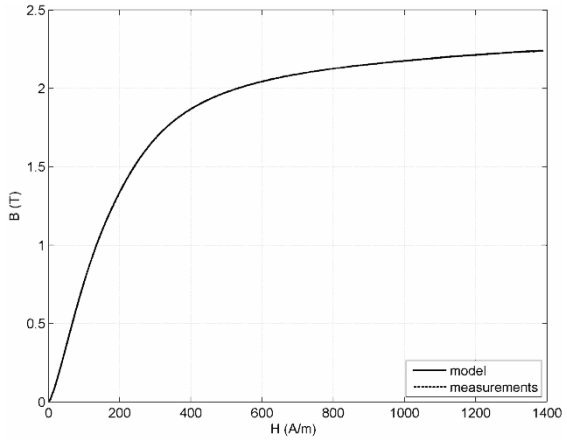

FIGURE 5. Comparison of the measurements and the approximation.

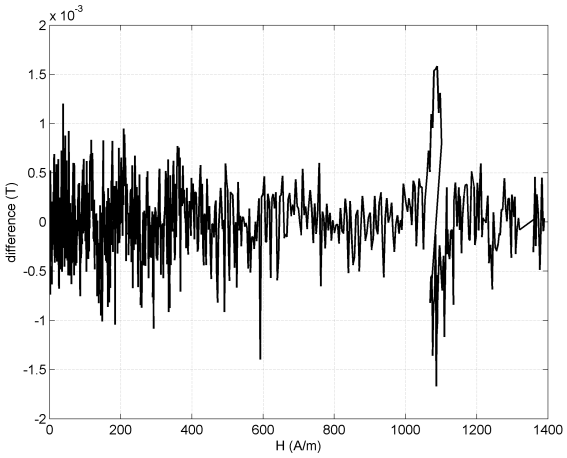

FIGURE 6. Difference between measurement and the model.

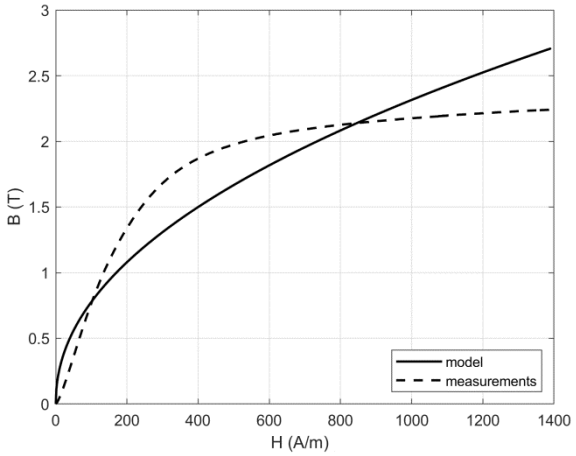

FIGURE 7. Simple exponential model.

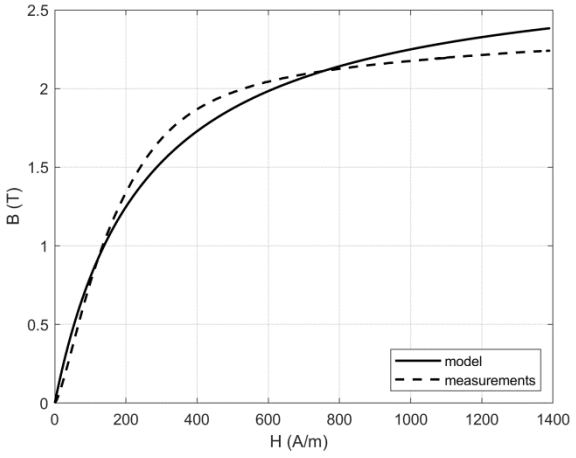

FIGURE 8. Froelich's model.

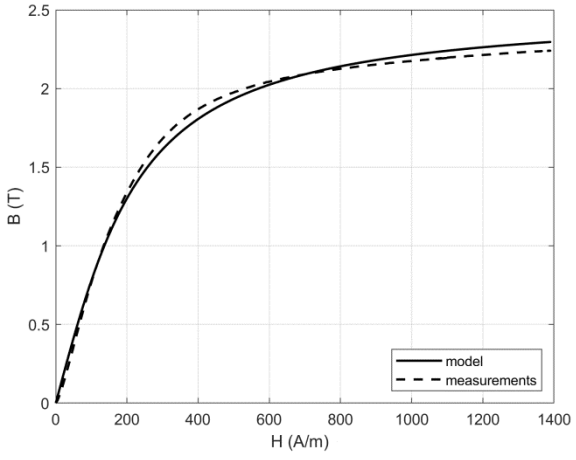

FIGURE 9. Inverse tangent approximation.

routine *pinv*. Fig. 5 presents the comparison of the measured data and the approximation results. To avoid an imaginary component in the model, produced by the numerical and round-off errors, the absolute value of the model is used in comparison. Since the two curves are indistinguishable, the Fig. 6 presents the difference between measurement and modeling.

V. COMPARISON WITH OTHER MODELS

The comparison of the proposed method and several established methods for the approximation of the initial B-H curve was based on the root-mean-square error (RMSE) criterion. RMSE is defined as

$$RMSE = \sqrt{\frac{\sum_{i=1}^{M}\left(b_i - \tilde{B}_i\right)}{M}} \tag{32}$$

where b_i denotes the approximated value given by the model, $\tilde{B}_i$ denotes the measured value, and M denotes the number of measured data points. The models used for the comparison were [26]:

a) Simple exponential model

$$B = aH^n \tag{33}$$

TABLE 2. Comparison of models.

Model	RMSE [T]
Simple exponential (a)	0.2346
Froelich's equation (b)	0.0951
Inverse tangent (c)	0.0456
Proposed model (complex exponential series)	$3.7313 \cdot 10^{-4}$

b) Froelich's equation

$$|\boldsymbol{B}| = \frac{|\boldsymbol{H}|}{\boldsymbol{a_1} + \boldsymbol{a_2}\,|\boldsymbol{H}|} \tag{34}$$

c) Representation by inverse tangent function

$$\boldsymbol{B} = \boldsymbol{a_1}\tan^{-1}(\boldsymbol{a_2}\boldsymbol{H}) \tag{35}$$

The nonlinear regression for models (a-c) was performed in MATLAB, applying the Levenberg-Marquardt algorithm with the MATLAB function *nlinfit*. The same set of the measured points was applied in the regression and the evaluation of all analyzed models. While Figs. 7-9 are giving a graphical comparison of the measurement data and models, Table 2 summarizes the quality of the modeling results based on the *RMSE* criterion. It is shown that the proposed model achieves the best fit (lowest RMSE), comparing to the analyzed established models. It should be noted that this is paid by the higher complexity of the proposed model.

VI. CONCLUSION

An accurate and simple least-squares solution is presented for the analytical approximation of single-valued *B-H* curves. Applying the Moore-Penrose pseudoinverse, a larger number of points in measurements can be used to obtain a lower order approximation. Due to the completeness of the orthogonal basis of the approximation, any desired accuracy can be achieved with increasing the number of terms. In line with the method of *B-H* curve modeling, an automated system for its measurement is presented, allowing the remote measurement through the arbitrarily number of points. In this way, a single PXI platform can be shared between several users with their own PC platforms. Thus, the measurements are performed remotely, while the approximation is obtained locally.

Using the model, the derivation of B with respect to H is easily obtained analytically, which is important in calculations of permeability and energy stored in the ferromagnetic material.

REFERENCES

[1] D. C. Jiles and D. L. Atherton, "Theory of ferromagnetic hysteresis," *J. Appl. Phys.*, vol. 55, no. 6, pp. 2115–2120, 1984.

[2] I. D. Mayergoyz, *Mathematical Models of Hysteresis*. Amsterdam, The Netherlands: Springer, 1991.

[3] T. W. Flateley and D. A. Henretty, "A magnetic hysteresis model," in *Proc. Flight Mechanics/Estimation Theory Symp.*, 1995, pp. 405–415.

[4] J. Ho Lee and D. Seek Hyun, "Hysteresis analysis for the permanent magnet assisted synchronous reluctance motor by coupled FEM and Preisach modelling," *IEEE Trans. Magn.*, vol. 35, no. 3, pp. 1203–1206, May 1999, doi: 10.1109/20.767165.

[5] J. B. Padilha, P. Kuo-Peng, N. Sadowski, and N. J. Batistela, "Vector hysteresis model associated to FEM in a hysteresis motor modeling," *IEEE Trans. Magn.*, vol. 53, no. 6, Jun. 2017, Art. no. 7402004, doi: 10.1109/TMAG.2017.2664582.

[6] D. Zhang, H.-J. Kim, W. Li, and C.-S. Koh, "Analysis of magnetizing process of a new anisotropic bonded NdFeB permanent magnet using FEM combined with Jiles-Atherton hysteresis model," *IEEE Trans. Magn.*, vol. 49, no. 5, pp. 2221–2224, May 2013, doi: 10.1109/TMAG.2013.2245499.

[7] J. V. Leite, K. Hoffmann, F. B. R. Mendes, N. Sadowski, J. P. A. Bastos, and N. J. Batistela, "Performance comparison between Jiles-Atherton and play vector hysteresis models on field calculation," in *Proc. IEEE Conf. Electromagn. Field Comput. (CEFC)*, Miami, FL, USA, Nov. 2016, p. 1, doi: 10.1109/CEFC.2016.7816376.

[8] H. Yoon, I. Kim, P. S. Shin, and C. S. Koh, "Finite element implementation of a generalized chua-type vector hysteresis model and application to iron loss analysis of three-phase transformer," *IEEE Trans. Magn.*, vol. 47, no. 5, pp. 1122–1125, May 2011, doi: 10.1109/TMAG.2010.2073684.

[9] X. Wang, D. Xie, B. Bai, N. Takahashi, and S. Yang, "3-D FEM analysis in electromagnetic system considering vector hysteresis and anisotropy," *IEEE Trans. Magn.*, vol. 44, no. 6, pp. 890–893, Jun. 2008, doi: 10.1109/TMAG.2007.916712.

[10] P. J. Leonard, D. Rodger, T. Karagular, and P. C. Coles, "Finite element modelling of magnetic hysteresis," *IEEE Trans. Magn.*, vol. 31, no. 3, pp. 1801–1804, May 1995, doi: 10.1109/20.376386.

[11] G. Miano, C. Serpico, L. Verolino, and C. Visone, "Comparison of different hysteresis models in FE analysis of magnetic field diffusion," *IEEE Trans. Magn.*, vol. 31, no. 3, pp. 1789–1792, May 1995, doi: 10.1109/20.376383.

[12] K. Hoffmann, J. P. A. Bastos, J. V. Leite, N. Sadowski, and F. Barbosa, "A vector Jiles–Atherton model for improving the FEM convergence," *IEEE Trans. Magn.*, vol. 53, no. 6, Jun. 2017, Art no. 7300304, doi: 10.1109/TMAG.2017.2660303.

[13] W. Li, I. H. Kim, S. M. Jang, and C. S. Koh, "Hysteresis modeling for electrical steel sheets using improved vector Jiles-Atherton hysteresis model," *IEEE Trans. Magn.*, vol. 47, no. 10, pp. 3821–3824, Oct. 2011.

[14] A. Benabou, S. Clénet, and F. Piriou, "Comparison of Preisach and Jiles-Atherton models to take into account hysteresis phenomenon for finite element analysis," *J. Magn. Magn. Mater.*, vol. 261, nos. 1–2, pp. 139–160, Apr. 2003.

[15] L. Janicke and A. Kost, "Convergence properties of the Newton-Raphson method for nonlinear problems," *IEEE Trans. Magn.*, vol. 34, no. 5, pp. 2505–2508, Sep. 1998, doi: 10.1109/20.717577.

[16] R. Das and D. A. Lowther, "Acceleration of field computation involving HTS," *IEEE Trans. Magn.*, vol. 49, no. 5, pp. 1785–1788, May 2013, doi: 10.1109/TMAG.2013.2242052.

[17] S. Niu, W. N. Fu, and S. L. Ho, "Nonlinear convergence acceleration of magnetic field computation," *IEEE Trans. Magn.*, vol. 51, no. 11, pp. 1–4, Nov. 2015, doi: 10.1109/TMAG.2015.2445342.

[18] M. L. Bash and S. Pekarek, "Analysis and validation of a population-based design of a wound-rotor synchronous machine," *IEEE Trans. Energy Convers.*, vol. 27, no. 3, pp. 603–614, Sep. 2012.

[19] G. M. Shane and S. D. Sudhoff, "Refinements in anhysteretic characterization and permeability modeling," *IEEE Trans. Magn.*, vol. 46, no. 11, pp. 3834–3843, Nov. 2010.

[20] J. Pearson, P. T. Squire, and D. Atkinson, "Which anhysteretic magnetization curve?" *IEEE Trans. Magn.*, vol. 33, no. 5, pp. 3970–3972, Sep. 1997, doi: 10.1109/20.619632.

[21] G. W. D. Spratt, M. Fearon, P. R. Bissell, A. Lyberatos, R. W. Chantrell, and E. P. Wohlfarth, "Interaction fields and the anhysteretic susceptibility of recording media," *IEEE Trans. Magn.*, vol. 24, no. 2, pp. 1895–1897, Mar. 1988, doi: 10.1109/20.11638.

[22] D. L. Atherton and V. Ton, "Effect of order of stress and field application on changes in anhysteretic magnetization," *IEEE Trans. Magn.*, vol. 26, no. 3, pp. 1157–1159, May 1990.

[23] J. P. Barton, "Empirical equations for the magnetization curve," *Trans. Amer. Inst. Elect. Eng.*, vol. 52, no. 2, pp. 659–664, Jun. 1933.

[24] R. E. Emery, "Rational and empirical formulÆ showing the relation between the magneto-motive force (H) and the resulting magnetization (B)," *Trans. Amer. Inst. Elect. Eng.*, vol. 9, no. 1, pp. 192–222, Jan. 1892.

[25] J. Brauer, "Simple equations for the magnetization and reluctivity curves of steel," *IEEE Trans. Magn.*, vol. MAG-11, no. 1, p. 81, Jan. 1975.

[26] F. Trutt, E. Erdelyi, and R. Hopkins, "Representation of the magnetization characteristic of DC machines for computer use," *IEEE Trans. Power App. Syst.*, vols. PAS–87, no. 3, pp. 665–669, Mar. 1968, doi: 10.1109/TPAS.1968.292178.
[27] W. A. Geyger, *Nonlinear-Magnetic Control Devices: Basic Principles, Characteristics and Applications*. New York, NY, USA: McGraw-Hill, 1964.
[28] M. El-Sherbiny, "Representation of the magnetization characteristic by a sum of exponentials," *IEEE Trans. Magn.*, vol. MAG-9, no. 1, pp. 60–61, Mar. 1973.
[29] W. K. MacFadyen, R. R. S. Simpson, R. D. Slater, and W. S. Wood, "Representation of magnetisation curves by exponential series," *Proc. Inst. Elect. Eng.*, vol. 120, no. 8, pp. 902–904, Aug. 1973.
[30] J. Rivas, J. Zamarro, E. Martin, and C. Pereira, "Simple approximation for magnetization curves and hysteresis loops," *IEEE Trans. Magn.*, vol. MAG-17, no. 4, pp. 1498–1502, Jul. 1981.
[31] P. Diez and J. P. Webb, "A rational approach to curve representation," *IEEE Trans. Magn.*, vol. 52, no. 3, Mar. 2016, Art. no. 7203604.
[32] G. F. T. Widger, "Representation of magnetisation curves over extensive range by rational-fraction approximations," *Proc. Inst. Electr. Eng.*, vol. 116, no. 1, pp. 156–160, 1969.
[33] G. Liu and X.-B. Xu, "Improved modeling of the nonlinear B-H curve and its application in power cable analysis," *IEEE Trans. Magn.*, vol. 38, no. 4, pp. 1759–1763, Jul. 2002.
[34] G. Arfken, *Mathematical Methods for Physicists*. New York, NY, USA: Academic, 1970.
[35] V. Alan Oppenheim, S. Alan Willsky, and S. Hamid, *Signals and Systems*, 2nd ed. London, U.K.: Pearson, 1997.
[36] L. Ljung, *System Identification: Theory for the User*. Englewood Cliffs, NJ, USA: Prentice-Hall, 1999.
[37] W. Parks, C. S. Burrus, *Digital Filter Design*. Hoboken, NJ, USA: Wiley, 1987.
[38] K. M. Tsui, S. C. Chan, and K. W. Tse, "Design of complex-valued variable FIR digital filters and its application to the realization of arbitrary sampling rate conversion for complex signals," *IEEE Trans. Circuits Syst. II, Exp. Briefs*, vol. 52, no. 7, pp. 424–428, Jul. 2005.
[39] K. Yao, "An alternative approach to the linear causal least-square filtering theory," *IEEE Trans. Inf. Theory*, vol. IT-17, no. 3, pp. 232–240, May 1971.
[40] *IEEE Standard Procedures for Magnetic Cores*, IEEE Standard 393-1991, 1992.
[41] M. Dadic, M. Jurcevic, K. Petrovic, B. Ivsic, and R. Malaric, "Automated system for the measurement of AC magnetization characteristics," in *Proc. 41st Int. Conv. Inf. Commun. Technol., Electron. Microelectron. (MIPRO)*, May 2018, pp. 151–155.
[42] P. Rupanagunta, J. S. Hsu, and W. F. Weldon, "Determination of iron core losses under influence of third-harmonic flux component," *IEEE Trans. Magn.*, vol. 27, no. 2, pp. 768–777, Mar. 1991.
[43] F. Overney, A. Rufenacht, J.-P. Braun, B. Jeanneret, and P. S. Wright, "Characterization of metrological grade analog-to-digital converters using a programmable Josephson voltage standard," *IEEE Trans. Instrum. Meas.*, vol. 60, no. 7, pp. 2172–2177, Jul. 2011.
[44] R. Rybski, J. Kaczmarek, and M. Koziol, "A high-resolution PXI digitizer for a low-value-resistor calibration system," *IEEE Trans. Instrum. Meas.*, vol. 62, no. 6, pp. 1783–1788, Jun. 2013.
[45] S.-C. Pei and J.-J. Shyu, "Design of arbitrary complex coefficient FIR digital filters by complex weighted least squares approximation," *IEEE Trans. Circuits Syst. II. Analog Digit. Signal Process.*, vol. 41, no. 12, pp. 817–820, Dec. 1994.
[46] M. Dadic and R. Zentner, "Wireless link modeling using complex FIR filters," in *Proc. 1st Int. Colloq. Smart Grid Metrol. (SmaGriMet)*, Apr. 2018, pp. 90–93.
[47] C. L. Lawson and R. J. Hanson, *Solving Least Squares Problems*. Upper Saddle River, NJ, USA: Prentice-Hall, 1974.
[48] A. Ben-Israel and T. N. E. Greville, *Generalized Inverses—Theory and Applications*, 2nd ed. Ottawa, ON, Canada: Canadian Mathematical Society, 2002.
[49] A. Papoulis, "Generalized sampling expansion," *IEEE Trans. Circuits Syst.*, vol. CAS-24, no. 11, pp. 652–654, Nov. 1977, doi: 10.1109/TCS.1977.1084284.
[50] H. J. Landau,"Sampling, data transmission, and the Nyquist rate," *Proc. IEEE*, vol. 55, no. 10, pp. 1701–1706, Oct. 1967, doi: 10.1109/PROC.1967.5962.
[51] P. L. Butzer, "Some recent applications of functional analysis to approximation theory," *Zum Werk Leonhard Eulers—Vorträge Euler-Kolloquiums*, vol. 1984. Berlin, Germany: Birkhäuser-Verlag, 1983, pp. 133–156.

MARTIN DADIĆ received the Dipl.Ing., M.Sc., and Ph.D. degrees in electrical engineering from the Faculty of Electrical Engineering and Computing, University of Zagreb, Zagreb, Croatia, in 1994, 1997, and 2000, respectively. From 1994 to 1995, he was a Telecommunications Engineer with T-Hrvatski Telekom, Zagreb. Since1996, he has been with the University of Zagreb, where he is currently a Full Professor of electrical engineering. From 2003 to 2005, he was an Adjunct Assistant Professor of electrical engineering with the University of Rijeka, Rijeka, Croatia. His current research interests include electromagnetic measurements, applied electromagnetics, and electroacoustics. He is a member of Croatian Society for Communication, Computing, Electronics, Measurement, and Control.

MARKO JURČEVIĆ (Member, IEEE) was born in Zagreb, Croatia, in 1980. He received the B.Sc. degree in information and communication technology and the Ph.D. degree in electrical engineering from the Department of Electrical Engineering Basics and Measurements, Faculty of Electrical Engineering and Computing, University of Zagreb, in 2003 and 2010, respectively.

He is currently an Assistant Professor with the University of Zagreb. His research interests include virtual instrumentation, and design and application of the remote measurements and calibration for electrical quantities and information security of measurement and automatization systems.

ROMAN MALARIĆ was born in Zagreb, Croatia, in 1971. He received the B.S. degree in radio communications, the M.Sc., and Ph.D. degrees from the University of Zagreb, Zagreb, in 1994, 1996, and 2006, respectively. Since 1994, he has been with the Department of Electrical Engineering Basics and Measurement, Faculty of Electrical Engineering and Computing, University of Zagreb, where he is currently a Full Professor. His current research interest includes the development of precise measurement methods for electrical quantities.